Adsorption of Hazardous Methylene Green Dye from Aqueous Solution onto Tin Sulfide Nanoparticles Loaded Activated Carbon: Isotherm and Kinetics Study

Marahel, Farzaneh*[+]

Department of Chemistry, Omidiyeh Branch, Islamic Azad University, Omidiyeh, I.R. IRAN

ABSTRACT: *In this research, a novel adsorbent, tin sulfide nanoparticles coated on activated carbon [SnS-NP-C] was synthesized by a simple, low cost and efficient procedure for the removal of methylene green from aqueous solutions. Subsequently, this novel material characterization and identification has been completed by different techniques such as TEM, FT-IR, and UV-Vis spectrometry analysis. In the batch experimental set-up, optimum conditions for quantitative removal of Methylene green by [SnS-NP-C] was attained following searching effect of variables such as adsorbent dosage (0.05-0.35 g), contact time (10-120 min), solution pH (6-10), and initial concentration of dye (10–60 mg/L) on the adsorption process was investigated. Optimum values were set at pH of 8.0, 0.25 g of [SnS-NP-C] at removal time of 50 min. Kinetic studies at the various adsorbent dosage and initial methylene green concentration show that maximum dye was sequestered within 10 min as a sort time. The adsorption of methylene green follows the pseudo-second-order rate equation in addition to interparticle diffusion model (with the removal of more than 99%) at all conditions. Equilibrium data fitted well with the Langmuir model at all amount of adsorbent, while maximum adsorption capacity was 14.22 mg/g for 0.2 g of [SnS-NP-C]. The present procedure is green and offers advantages such as shorter reaction time, simple workup, and high percentage removal.*

KEYWORDS: *Adsorption; Methylene green; Tin sulfide nanoparticles loaded activated carbon; Kinetics; Isotherm.*

INTRODUCTION

The use of artificial chemical dyes in various industrial processes has increased considerably over the last few years. Some areas where these chemicals are frequently used are paper and pulp manufacturing, plastics, dyeing of cloth, leather treatment, printing, etc. Industrial wastewaters containing such dyes are generally discarded as effluents. Since some of these dyes are toxic, their removal from industrial effluents is a major environmental problem [1–3]. Wastewaters of these industries contain dye with metals, salts, and other chemicals that may be toxic to the aquatic environment. Charges of such wastes in water sources cause damage to ecological balance and affects photosynthetic activity [1]. Hence, the presence of dyes in wastewaters is a major

*** To whom correspondence should be addressed.*
+ E-mail: farzaneh marahel@yahoo.com
1021-9986/2019/5/129-142 14/$/6.04

the environmental problem as they are generally resistant to degradation by biological treatment methods. Textile wastewater contaminated with azo reactive dyes needs to be treated by physical and chemical means before discharging. Azo dyes account for about 70% of dyes used in the textile industry, and since dyes are stable, recalcitrant, colorant, and even potentially carcinogenic and toxic, their release into the environment poses serious environmental, aesthetical and health problems [4]. The treatment of dye wastewater becomes more important than ever for the environment. Many technologies were applied to treat dye wastewater, such as biological treatment [5], electrocoagulation [6], chemical oxidation [7], membrane filtration [8], nanoparticles [9], photocatalytic degradation [10], and adsorption [11]. Amongst, adsorption technology due to its effectiveness, high efficiency, economy, and no secondary pollution are very interested. The main criterion is the selection of suitable sorbent that favored by using nano-structures loaded on activated carbon. Carbon-based materials due to their high surface area, porous structure, large adsorption capacities, fast adsorption kinetics are a good candidate and alternatives for loading nanomaterial [12, 13]. The nanoparticles have very interesting physicochemical properties, such as ordered structure with high aspect ratio, ultra-lightweight, high mechanical strength, electrical and thermal conductivity, metallic or semi-metallic behavior, and medium-specific surface area [14-17]. Being one of the most important nanomaterials materials, soft chalcogenides metal sulfide is very useful indifferent technological fields such as soft adsorption. Among those materials, tin sulfide has attracted research attention in recent years, because of their very important properties such as their ability to form several binary sulfides, like SnS, Sn_2S_3, Sn_3S_4, and SnS_2, which this is due to the coordination features of polyvalent tin and sulfur. Tin monosulfide (SnS), and tin disulfide (SnS_2) seem to be the most important and the most studied compounds, which due to their low bandgap they are soft molecules. Stannous sulfide (SnS), is a binary polymorphic semiconductor with a cubic, zinc-blende and orthorhombic structure. The orthorhombic double-layered crystalline structure is stable in ambient conditions. In this structure, the layers of S and Sn atoms are founded together by the weak van der Waals force [18]. Besides, SnS exhibits a very useful band gap varying in the range (1.2–1.5 eV), and a high absorption coefficient. Therefore it can be used in the adsorption process as a soft adsorbent for removal of the soft analyst (soft analytes: low bandgap analytes. Therefore, SnS can be used as a good modifier nanostructure for the modification of activated carbon [19]. Methyl green as soft dyes (with medium bandgap conformational entropy) tends to adsorb to surfaces under a wider variety of conditions by permitting rearrangements of the molecular structure upon the adsorption. As a consequence, it is generally accepted that while semisoft dyes can adsorb to a variety of surfaces (even under unfavorable electrostatic conditions), the interaction of hard dyes requires a more careful selection of the experimental conditions (surface charge, solution pH, ionic strength, etc.) [20]. Therefore, the selection of these materials for adsorption of the soft dyes can be assisted for dyes adsorbed to the solid surface of soft adsorbent by a combination of (mostly) electrostatic, H bond, soft-soft interaction and other hydrophobic and or hydrophilic forces. Finally, and depending on the structure, soft dyes molecules can relax and spread to maximize the number of interaction points with the soft/soft adsorbent surface [21].

EXPERIMENTAL SECTION

Materials

All chemicals including NaOH, HCl, HNO_3, KOH, KCl, NaCl, methylene green, activated carbon and other reagents with the highest purity available were purchased from Merck, Darmstadt Germany. Methylene green (Fig. 1) was used as received without any further purification. A stock solution of methylene green was prepared by dissolving 10 mg in 100 mL distilled water and its working solutions were prepared by successive dilutions of the stock solution. The methylene green concentration was determined at 525 nm using Jusco UV-Visible spectrophotometer model V-530 (Tokyo, Japan) based on the respective calibration curve obtained at the same conditions. pH/Ion meter model-686 (Metrohm, Switzerland, Swiss), international ASTM sieves and Stirrer model (UKA Switzerland, Swiss). Absorption measurements were carried out on a Perkin Elmer Lambda 25 spectrophotometer (Tokyo, Japan) using a quartz cell with an optical path of 1 cm. The morphology and electron diffraction patterns of the SnS nanoparticles were determined by Hitachi H-800 TEM at an operating

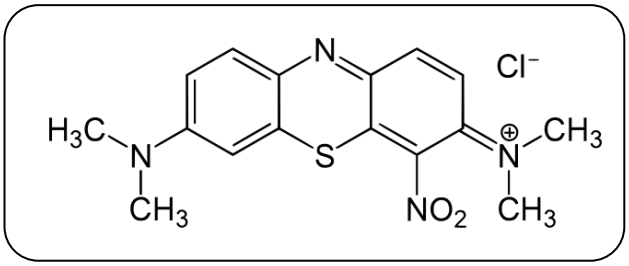

Fig. 1: Structure of Methylene green.

the voltage of 200 kV. Fourier Transform InfraRed (FT-IR) analysis for characterization of the adsorbent was performed using a KBr disk (Shimadzu FTIR-8300 spectrophotometer, Shimadzu Co., Tokyo, Japan).

Batch adsorption experiments

The influence of variables including pH, adsorbent dosage, contact time and initial dye concentration on the adsorptive removal of methylene green was investigated by batch experiments. In each experimental run onto [SnS-NP-C, 100 mL of 10 mg/ L of NFR in 250 mL Erlenmeyer flasks was agitated on stirrer at 400 rpm at room temperature and obtained experimental data at various times, concentration was fitted to different models to evaluate and calculate the kinetics and isotherm parameters of the adsorption process. The solution pH was adjusted via the addition of dilute aqueous solutions of HCl and/or NaOH (0.1 M). The Methylene green removal percentage was calculated using the following equation [25]:

$$\%\ \text{Dye removal} = \left(\left(C_0 - C_t\right)/C_0\right)\times 100 \qquad (1)$$

Where C_0 (mg/L) and C_t (mg/L) are the dye concentration at initial and after time t respectively and the equilibrium adsorption capacity of Methylene green was calculated according to equation [26]:

$$q_e = \left(C_0 - C_e\right)V/W \qquad (2)$$

Where C_0 (mg/L) and C_e (mg/L) are the initial and equilibrium dye concentrations in solution, respectively, V is the volume of the solution (L), and W is the mass (g) of the adsorbent.

Preparation of SnS nanoparticles coated on AC

To stabilize the tin sulfide nanoparticles on activated carbon, 0.1 g of the nanoparticles with 1.0 g of activated carbon was mixed in ethanol for 24 h. Finally, products as SnS-NPs-AC were filtrated, washed and dried at 85 °C for 12 h.

RESULTS AND DISCUSSION

Characterization of [SnS-NP-AC]

The characteristic functional groups of the adsorbent were investigated using FT-IR spectra. The FT-IR spectrum of present sorbent shows the high intensity of OH vibrations and lower contribution of CH_2 and CH_3 asymmetric and symmetric stretching vibrations. Two strong peaks observed in the range between 2359cm^{-1} and 2338cm^{-1} are assigned to asymmetric C–H bands and symmetric C–H bands, respectively, present in SnS and AC groups. Stretching vibration band around 1651cm^{-1} is assigned to carbonyl C=S group present in aldehyde, ester, ketone and acetyl derivatives. The strong band at 1651cm^{-1} may be due to C= C band. FT-IR spectra for SnS in Fig. 2 (b) the stretching vibration band around 1185cm^{-1} is assigned to Sn=S and S=O groups present in thiocarbonyl and sulfonyl chloride 2 derivatives. One strong peak observed in the range 827cm^{-1} is assigned to C-Cl or C-H (out of plan) bands, respectively, present in alkyl halides and aromatics groups. FT-IR spectra for Tin oxide coated on activated carbon in Fig. 2 (c) the Vibratory band at 2329cm^{-1} may be due to Sn-H silane miscellaneous band. Stretching vibration band around 1160 cm^{-1} is assigned to C=S and S=O groups present in thiocarbonyl and sulfonyl derivatives. One strong peak observed in the range 834cm^{-1} is assigned to C-Cl or C-H (out of plan) bands, respectively, present in alkyl halides and aromatics groups and the strong band at 552 cm^{-1} may be due to C-Br band, present in alkyl halides groups. TEM image of the SnS-NP-AC in Fig. 3 Show homogeneous structure and appearance of different pores in the adsorbent structure that make possible it as useful sites for adsorption. TEM analysis of SnS-NP shows the spherical and low small size of SnS-NP with homogenous size distribution. TEM image shows that the size was between 10–100 nm.

Analytical methods

Concentrations of the dye were measured at the wavelength of its maximum absorbance (λ_{max}) that was determined by the Jasco UV-Vis spectrophotometer model V-530. The final dye concentration was determined spectrometric ally corresponding to λ_{max} of the dye using the Beer-Lambert equation:

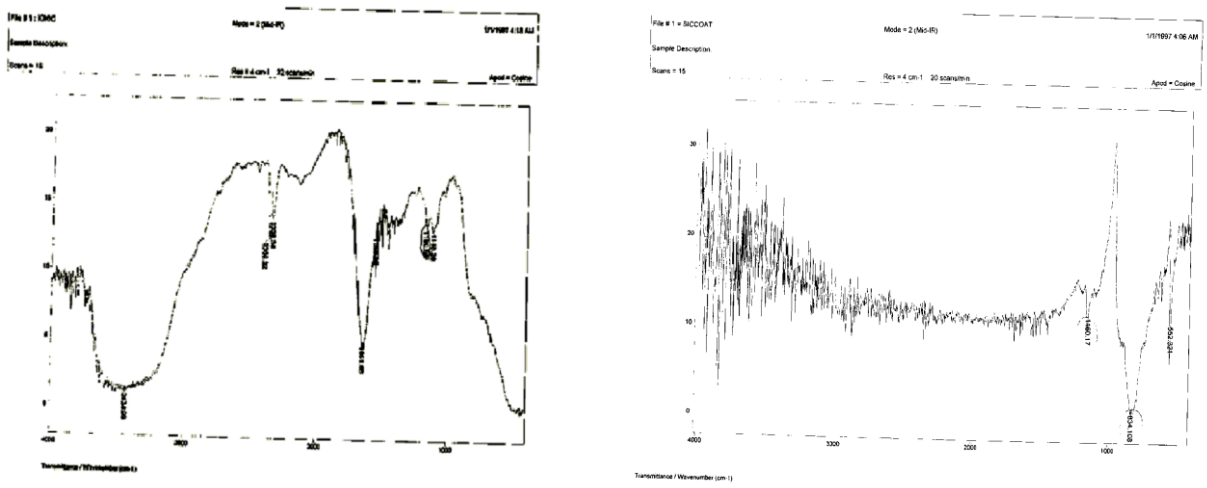

Fig. 2: (a) FT-IR spectrum of Methylene green (b) FT-IR spectrum of SnS nanoparticle

$$\text{Absorbance} = l \; {}_{S}(\qquad (3)$$

Where: ϖ is the molar absorptivity, C_S the concentration of sample and l the thickness of absorbing medium (1cm).

The wavelength of maximum absorbance (λ_{max}) and calibration curve

To determine the wavelength of maximum absorbance for the Methylene green different concentrations of dye solutions were prepared depending on the characteristic intensity of the dye color and sensitivity of the instrument for the dye. The wavelengths of maximum absorbance (λ_{max}) of the solutions were determined for the dye and calibration curve are constructed to determine the initial and final concentration. To this end a calibration curve was prepared by dissolving an amount of the dye to make 10 mg/L of dye solution. Then the other series of solutions are made by taking the corresponding volume of the previously concentrated dye solutions using distilled water and measuring their absorbance at their respective λ_{max}. The concentration and measured absorbance for each dye solution is used to construct the calibration curve. The wavelength of maximum absorbance is indicated for concentrations of dye used to construct the calibration curve for dye, Fig. 4 shows in the calibration curve of Methylene green.

Effect of system pH on Methylene Green Uptake

The pH of the system exerts a profound influence on the ability of adsorbent surface for interaction and dye molecule tendency for binding to a solid surface. Solution pH is an important parameter that affects the adsorption of dye molecules. These phenomena presumably are due to its influence on the surface properties of the adsorbent and ionization/ dissociation of the adsorbate molecule [27, 28]. The effect of the initial pH of the solution on the adsorption of Methylene green onto [SnS-NP-AC] surfaces was assessed at different pH values, ranging from 6.0 to 10.0. The initial concentrations of both dye and adsorbent dosage were set at 10 mg/L, respectively. The experiments were performed in a batch technique and each solution was stirred for 30 min. The results of this experiment are summarized in Fig. 5 and show that the initial pH of the sample solution could significantly affect the extent of adsorption of both dyes. Since the populations of negatively charged nanoparticles are expected to be increased by increasing pH, the percent removal of dye is firstly increased as long as the dye molecules are present in their positive or neutral form which is the case in the pH values 8.0. Fig. 5 shows the variations in the Methylene green removal from wastewater at different solution pH. It is evident, that the maximum removal of methylene green is observed at pH 8.

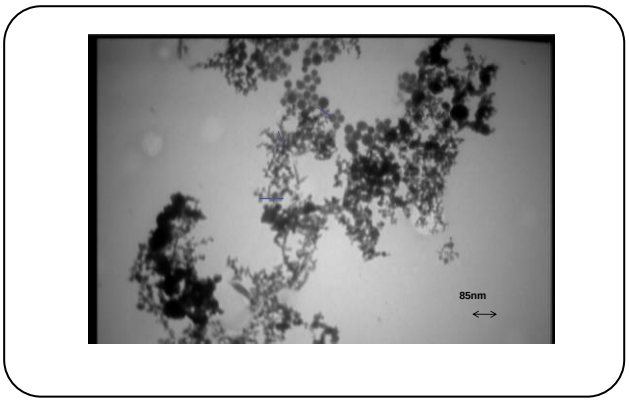

Fig. 3: TEM image of SnS nanoparticles.

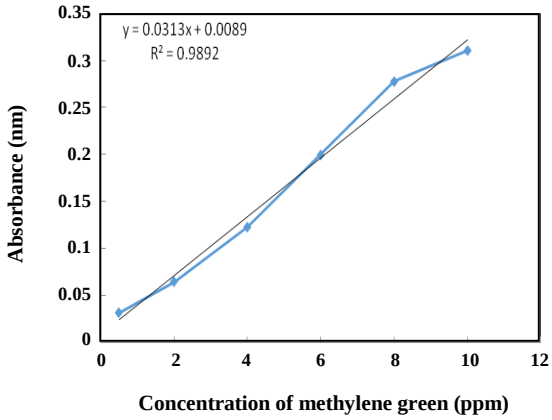

Fig. 4: Calibration curve for Methylene green at λ_{max} .

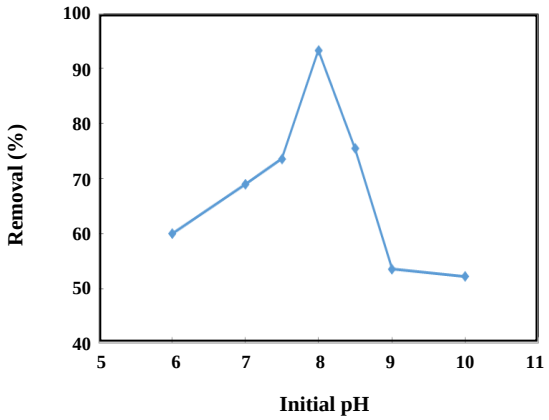

Fig. 5: Effect of initial pH on adsorption of Methylene green (10 mg/L) onto [SnS-NP-AC] (0.25 g of adsorbent, 10 mg/L) at room temperature (27±2 ◦C), agitation speed 400 rpm for the maximum contact time required to reach the equilibrium (30 min).

Effect of adsorbent dosage

The effect of [SnS-NP-AC] dosage on removal of Methylene green was investigated using a batch technique by adding a known quantity of the adsorbent, in the range of 0.05–0.35 g of its powdered form, into individual beakers containing 100 mL of the dye solution. After the mixing time elapsed, the SnS nanoparticles were magnetically separated and the solution was analyzed for the residual dye. For all measurements, the initial dye concentrations and the pH of the solutions were fixed at 10 mg/L and 8, respectively. Results shown in Fig. 6 indicate that 99% of Methylene green were removed from their aqueous solutions when an initial dosage of 0.35 mg [SnS-NP-AC] was used. The percent removal of both dyes increased with increasing [SnS-NP-AC] up to the dosage of 0.25 g and eventually reached a value of 99.8% for each one. This observation can be explained by the greater number of adsorption sites made available for dye molecules at greater [SnS-NP-AC] dosages [29]. Further increase of 0.25 g of the adsorbent dosage did not affect the removal of dye. Hence, the optimum dosage of [SnS-NP-AC] for removing both methylene green from their solutions was found to be 0.25 g.

Effect of contact time

The contact time between adsorbate and adsorbent is one of the most important design parameters that affect the performance of adsorption processes. The effects of both contact and stirring periods on the performance of [SnS-NP-AC] for adsorption Methylene green were investigated individually. The [SnS-NP-AC] dosage of 0.25 g and a solution pH of 8 were used for this investigation. The initial dye concentration for all test solutions was 10 mg/L.

Fig. 7 shows removal efficiencies for both dyes as a function of stirring time ranging between 10 and 30 min. These data indicate that the adsorption process started immediately upon adding the [SnS-NP-AC] powder to both solutions. The removal efficiency for Methylene green rapidly increased from 64% in the first 10 minutes of contact to a value of 99.8%, where the equilibrium condition was attained, as the stirring was increased to 30 min. Thus, the contact time required to achieve equilibrium and complete adsorption for both of the tested model dye was the same. Therefore, the optimum contact time between the sample solution

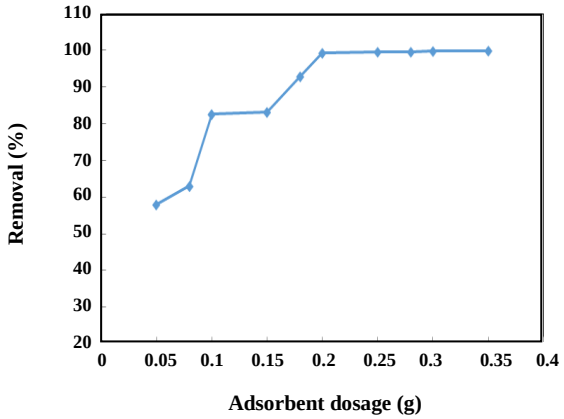

Fig. 6: Effect of adsorbent dosage on Methylene green removal in the range of 0.05-0.35 g at (pH 8.0, initial dye concentration of 10 mg/L, the contact time of 50 min, agitation speed: 400 rpm, temperature: 27±2 ◦C).

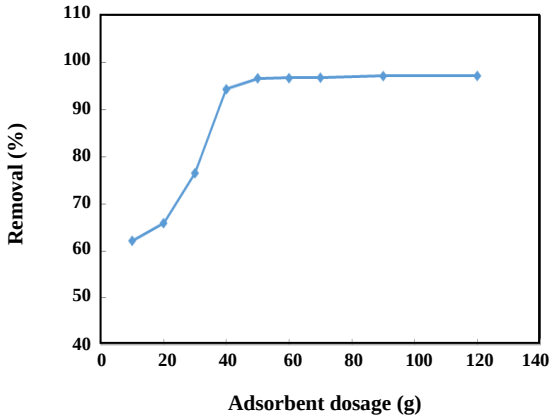

Fig. 7: Effect of contact time on the removal of Methylene green onto [SnS-NP-AC] in concentration 10 mg/L of Methylene green at pH 8.0, 0.2 g of [SnS-NP-AC].

and [SnS-NP-AC] was considered to be 50 min. The shorter the contact time in an adsorption system, the lower would be the capital and operational costs for real-world applications. The contact time obtained in this study was found to be shorter than most of the reported values for dye adsorption by other adsorbents [30, 27].

Effect of initial dye concentration on adsorption of Methylene green

The effect of Methylene green concentration in the range of 10–60 mg/L on its adsorption by [SnS-NP-AC] was investigated and the amount and percentage of Methylene green removal at different initial concentrations (10, 20, 30, 40, 50 and 60 mg/L) were depicted in Fig. 8. As shown, the actual amount of the Methylene green uptake increased at higher initial dye concentrations, while the removal percentage significantly decreased with further increase in initial dye concentrations that emerged from saturation and occupation of the available sites on the adsorbent.

It seems that at higher Methylene green concentration, due to an increase in its molecule competition for the low vacant reactive sites the adsorption of the process will increasingly slow down. This phenomenon related to a decrease in the mass gradient between the solution and adsorbents (driving force for the transfer of dye molecules from the bulk solution to the particle surface). At lower dye concentrations, solute to adsorbent vacant sites ratio is high and causes an increase in color removal [28].

Ionic strength

Since the presence of any ion could affect on the hydrophobic and electrostatic interaction between dye and surface of [SnS-NP-AC] as adsorbent, the effect of solution ionic strength on the removal of Methylene green was investigated under optimum experimental conditions in batch technique. A selected concentration of NaCl in the 0.1-0.6 mol/L was added to individual beakers containing 100 mL of the tested dye solution (Fig. 9). The resulting suspension was immediately stirred with a magnetic stirrer for 50 min. After the mixing time elapsed, the [SnS-NP-AC] nanoparticles were magnetically separated and the solution was analyzed for the residual dye. The adsorption capacities of [SnS-NP-AC] for Methylene green were not significantly affected with increasing NaCl concentration this indicates that Cl^- ions do not compete with the negative charge groups of the dye molecules for adsorption onto [SnS-NP-AC] surface.

Adsorption equilibrium

Adsorption isotherms study is the preliminary step to design efficient adsorption systems that empirically is applicable to explain the equilibrium relationship between equilibrium Methylene green concentration (adsorbent and removal in solution). The equilibrium adsorption of Methylene green (qe versus Ce) onto both adsorbents

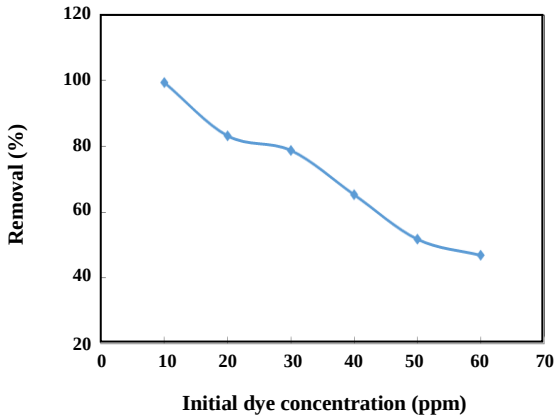

Fig. 8: Effect of initial dye concentration on the adsorption of Methylene green in the range of 10-60 mg/L and 0.2 g adsorbent at (pH 8.0, the contact time of 50 min, agitation speed: 400 rpm, temperature: 27±2 ◦C).

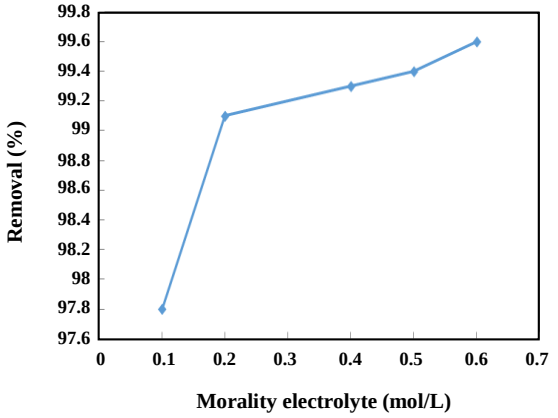

Fig. 9: Effect of solution ionic strength on the removal of Methylene green

was investigate at some different adsorbent mass to achieve conditions for the real applicability of both adsorbents in wastewater treatment. The experimental equilibrium data of adsorption of Methylene green was fitted to conventional isotherm models such as Langmuir, Freundlich, Temkin, and Dubinin–Radushkevich isotherms with known assumption presented in Table 1 for [SnS-NP-AC]. It was found that for both adsorbent the adsorption capacity reduced.

Langmuir adsorption isotherm model

The well known linear form of Langmuir's adsorption isotherm equation (Eq. (4)) was applied for the Methylene green– [SnS-NP-AC] system.

$$C_e/q_e = 1/K_a Q_m + C_e/Q_m \quad (4)$$

Where q_e is the number of moles of solute adsorbed per unit weight at concentration C (mol/g), C_e is the equilibrium molar concentration of the dye (mol/L), Q_m is the maximum adsorption capacity and b is the energy of adsorption. At all the temperatures, the $1/C_e$ versus 1/qe graphs give straight lines with appreciable values of the regression coefficient (R^2) close to unity, verifying the Langmuir adsorption model and ascertaining that monolayer formation is taking place during the adsorption of Methylene green over the surface of [SnS-NP-AC]. Based on gradient and interception of these straight lines, Langmuir constant 'b' and number of moles of the dye adsorbed per unit weight of the adsorbent (Q_m) have been evaluated and presented in Table 1. To confirm this result, the favorable or unfavorable Methylene green adsorption onto Langmuir model was judged by calculation of the separation factor (RL) as follow [31, 32].

$$RL = 1/(1 + K_a C_0) \quad (5)$$

Where k_a (L/mg) is the Langmuir constant and C_0 (mg/L) is the initial concentration. The adsorption process can be determined as favorable when the RL value lies between 0 and 1. It was found that for all adsorbent dosages and initial Methylene green concentrations the RL value is lower than 1, suggest the favorable adsorption and good fitness of the Langmuir model to explain experimental data. On the other hand, the increase in RL value with rising initial Methylene green concentration and adsorbent dosage show a high tendency of Methylene green for adsorption onto [SnS-NP-AC].

Freundlich adsorption isotherm model

The following equation describing the Freundlich model for the adsorption of solutes from a liquid to a solid surface was applied for the present adsorption system:

$$\mathrm{Ln}\, q_e = \ln K_F + (1/n) \ln C_e \quad (6)$$

Where *qe* is the amount adsorbed (mol/g), C_e is the equilibrium concentration of the adsorbate (M), K_F and n the Freundlich constants, are related to adsorption capacity and adsorption intensity, respectively. Straight lines with regression coefficients close to unity were obtained in ln C_e versus log qe, graph, and values of constants K_F and n derived from the intercepts and

Table 1: Isotherm constants of Methylene green adsorption onto [SnS-NP-AC].

[SnS-NP-AC] (g)				
Isotherm	Equation	Parameters	0.2	0.25
Langmuir	$C_e/q_e = 1/K_aQ_m + C_e/Q_m$	Q_m (mg/g)	14.22	11.76
		K_a (L/mg)	0.762	0.416
		RL	0.021-0.116	0.038-0.194
		R^2	0.9941	0.9857
Freundlich	$Ln\ q_e = ln\ K_F + (1/n) ln\ C_e$	1/n	0.1702	0.2659
		K_F (L/mg)	7.807	4.653
		R^2	0.9543	0.9630
Temkin	$q_e = B_l\ ln\ K_T + B_l\ ln C_e$	B_l	1.458	1.831
		K_T (L/mg)	345.02	13.41
		R^2	0.9143	0.9738
Dubinin and Radushkevich	$Ln\ q_e = ln\ Q_s - K\varepsilon^2$	Q_s (mg/g)	11.87	9.45
		K	2E-08	1E-07
		E (J/mol)= $1/(2K)^{1/2}$	5000	2236.07
		R^2	0.7919	0.8594

the slopes of these straight lines are presented in Table 1. The verification of the Freundlich model confirms the homogeneous nature of adsorption of Methylene green over the surface of [SnS-NP-AC] at each temperature [33].

The Temkin isotherm

Judgment for suitability of each model for the representation of methods applicability for an explanation of experimental data is according to R^2 value. Although Langmuir and even Freundlich model have reasonable and acceptable R^2 values, the applicability of other models such as Tempkin isotherm has commonly been applied in the following linear form [34, 35]: The Tempkin isotherm Eq. (7) can be simplified to the following equation:

$$q_e = B_l \ln K_T + B_l \ln C_e \quad (7)$$

Where $B_l = (RT)/b$ is related to the heat of adsorption, *T* is the absolute temperature in Kelvin and *R* is the universal gas constant, 8.314 (J/mol.K) [31,32, 34]. The adsorption data were analyzed according to the linear form of the Temkin isotherm Eq. (7). Examination of the data shows that the Temkin isotherm is efficiently applicable for fitting the Methylene green adsorption onto [SnS-NP-AC]. The linear isotherm constants and coefficients of determination are presented in Table 1. The heat of Methylene green adsorption onto [SnS-NP-AC] was found to increase from 1.485 to 1.831 kJ/mol with an increase in [SnS-NP-AC] dose from 0.2 to 0.25 g. The correlation coefficients R^2 obtained from Temkin model were comparable to that obtained for Langmuir and Freundlich equations, which explain the applicability of Temkin model to the adsorption of Methylene green on to [SnS-NP-AC].

D–R adsorption isotherm model

To identify the nature of the ongoing adsorption process, following D–R adsorption isotherm model was applied [36, 37]:

$$\ln q_e = \ln Q_s - K\varepsilon^2 \quad (8)$$

Where *qe* is the amount of the dye adsorbed per unit weight of the adsorbent (mg/g), Q_s is the maximum sorption capacity provided by the intercept (μmol/g), K (mol^2/J^2) is the activity coefficient related to mean sorption energy, and ε (Eq. (9)) is Polanyi potential [37, 38].

$$\varepsilon = RT\ln\left(1+\frac{1}{C_e}\right) \quad (9)$$

Where *R* is the universal gas constant and *T* is the temperature in Kelvin. The activity coefficient (K) and the adsorption capacities (ln Q_s) were evaluated from the slopes and intercepts of the plot ln qe versus ε^2 at 25 °C and these results are depicted in Table 1. The mean sorption energy (E) was calculated from the values of K by the following expression [38]:

$$E = 1/\sqrt{2K} \quad (10)$$

Based on values of *K*, obtained from the D–R isotherm graph, values of mean sorption energy were calculated at each temperature.

Adsorption kinetics

Several steps can be used to examine the controlling mechanism of the adsorption process such as chemical reaction, diffusion control, and mass transfer. Generally, kinetic models are used to test experimental data of Methylene green adsorption. The kinetics of Methylene green adsorption onto [SnS-NP-AC] is required for selecting optimum operating conditions for the full-scale batch process. The kinetic parameters, which are helpful for the prediction of adsorption rate, give important information for designing and modeling the adsorption processes. Thus, the kinetics of Methylene green adsorption onto [SnS-NP-AC] were analyzed using pseudo-first-order [39], pseudo-second-order [40], Elovich [41, 42] and intraparticle diffusion [43, 31] kinetic models. The conformity between experimental data and the model predicted values was expressed by the correlation coefficients (R^2, values close or equal to 1). The relatively higher value is the more applicable model to the kinetics of Methylene green adsorption onto the adsorbent. The pseudo-first-order and the pseudo-second-order adsorption models were used to test the experimental data. The two kinetic models equations are given as follow:

Pseudo-first-order equation:

$$\mathrm{Log}(q_e - q_t) = \log(q_e) - (K_1/2.303)t \quad (11)$$

Pseudo-second-order equation:

$$t/q_t = 1/k_2 q_e^2 + (1/q_e)t \quad (12)$$

Where *qe* and *qt* are the amounts of Methylene green adsorbed on adsorbent (mg/g) at equilibrium time and at time *t* (min), respectively; K_1 is the rate constant of pseudo-first-order adsorption (min^{-1}), K_2 is the rate constant of second-order adsorption (g/(mg min)). To testify the applicability of these two models, six initial dye concentrations, 10, 20, 30, 40, 50 and 60 mg/L were applied. The results of the kinetic parameters are listed in Table 2. Based on the correlation coefficients (R^2=0.9979) the adsorption of Methylene green is best described by the pseudo-second-order equation, suggesting that the rate-limiting step may be the adsorption mechanism but not the mass transport [44].

Intra-particle diffusion

In a batch system under rapid stirring, there is a possibility that the transport of the adsorbate from the solution into the bulk of the adsorbent is the rate-controlling step. This possibility was explored using the intraparticle diffusion model [45]. The initial rate of intraparticle diffusion is given by the following equation:

$$q_t = K_{id}t^{1/2} + C \quad (13)$$

Where *qt* is the amount of dye on the surface of the sorbent at time t (mg/g), K_{id} is the intraparticle diffusion rate constant [(mg/g) $min^{1/2}$], t is the time (min) and *C* is the intercept (mg/g). According to Eq. (13), a plot of qt versus $t^{1/2}$ should be a straight line when the adsorption mechanism follows the sole intraparticle diffusion process. Some authors have reported that it is essential for the plots to cross the origin if the intraparticle diffusion is the sole rate-limiting step [46, 47]. In the present study, the plot does not cross through the origin instead, the plot of qt against $t^{1/2}$ tends to present a multi-linear behavior, which indicates that two or more steps occur in the adsorption processes, involving instantaneous adsorption on the external surface, intraparticle diffusion or gradual adsorption being the rate-controlled stage, and the final equilibrium stage

Table 2: Kinetic parameters of Methylene green adsorption onto [SnS-NP-AC] Conditions: 0.2 g adsorbent over 10-60 mg/L at optima conditions of other variables.

Parameter values: Concentration dye (ppm)							
Models	parameters	10	20	30	40	50	60
First order kinetic model: $\text{Log}(q_e-q_t)=\log(q_e)-(K_1/2.303)t$	K_1	0.0624	0.0677	0.0414	0.0444	0.0330	0.0534
	qe (cal)	2.525	5.832	10.358	11.209	1.443	20.831
	R^2	0.8700	0.7415	0.8624	0.8406	0.9755	0.9165
Second order kinetic model: $t/q_t=1/k_2q_e^2 + (1/q_e)t$	K_2	0.024	0.0145	0.0076	0.008	0.036	0.0036
	qe (cal)	5.285	9.14	11.90	12.02	2.84	16.64
	R^2	0.9934	0.9968	0.9951	0.9955	0.9979	0.9917
	H	0.675	1.212	1.08	1.158	0.294	1.008
Intraparticle diffusion $q_t=K_{id}\, t^{1/2}+C$	K_{dif}	0.2568	0.3913	0.5180	0.5039	0.1325	0.8291
	C	2.5527	4.8471	5.6707	5.9781	1.3362	6.6850
	R^2	0.7352	0.8459	0.9902	0.9902	0.9073	0.9485
Elovich $q_t= 1/\beta \ln(\alpha\beta) + 1/\beta \ln(t)$	B						
	R^2	0.8338	0.9140	0.9708	0.9709	0.9508	0.9370
Experimental adsorption capacity	qe(exp)	4.87	8.50	11.15	11.30	2.65	15.05

where the intraparticle diffusion slows down due to the extremely low solute concentration in solution. This phenomenon corresponds to the study of [48]. Since the first stage (external surface adsorption) is completed fast and is less apparent, only the second stage (intraparticle diffusion) and the third stage (equilibrium) are demonstrated. On the other hand, the intercept of the plot reflects the boundary layer effect. Larger the intercept, greater is the contribution of the surface sorption in the rate-limiting step. Corresponding model fitting parameters (Table 2) indicates the adsorption mechanism also follows the intraparticle diffusion process.

Elovich equation

In this model with a known equation presented in literature, α is the initial adsorption rate [(mg/g) min] and β is the desorption constant related to the extent of surface coverage and activation energy for chemisorptions (g/mg). The parameters (1/β) and (1/β) ln (αβ) can be calculated from the slope and intercept of the linear plot of q_t versus ln (t). The obtained R^2 value of this model was 0.9708 for Methylene green initial concentration in the range of 10–60 mg/L on [SnS-NP-AC] adsorbent (Table 2). The parameter 1/β is related to the number of sites available for adsorption while (1/β) ln (αβ) is the adsorption quantity when ln *t* is equal to zero. Adsorption quantity at 1 min helps understand the adsorption behavior of the first step [49-51].

Adsorption mechanism

It has been reported that ionic bonding between the positively charged functional groups of methyl green and negatively charged of adsorbent at pH 8 (optimum pH) can be formed. Also, the bond between S and O atom in adsorbent and H atoms in methyl green can be a probable mechanism for understudy dye adsorption. The above mentions indicated that electrostatic interaction was one of the mechanisms for the adsorption of methyl green. In another word, adsorption behavior and adsorption mechanism, especially the affinity of SnS-NPs for specific pollutants depended on Lewis acid-base (between adsorbent and adsorbate) character. In SnS-NPs as soft, have a narrow bandgap energy (~1.4 eV), thus it was a soft adsorbent. Therefore, the selection of this material for adsorption of the soft methyl green can be assisted for dye adsorbed to the solid surface of soft adsorbent by a combination of (mostly) electrostatic, H bond, soft-soft interaction and other hydrophobic

Table 3: Comparison with literature.

Process	Dye	Concentration (mg/L)	Adsorbent	Adsorbent mass (g/L)	Time (min)	Efficiency
Adsorption [52]	Methyl Green	5	Loofah fiber	0.4	250	75.8%
Adsorption [53]	Methyl Green	100	$NiFe_2O_4$-CNTs	1.4	120	56.19%
Adsorption [54]	Methyl Green	25	Amberlite XAD-2 resin	0.014	150	95%
Adsorption [55]	Methyl Green	100	Pomegranate Peels	1.0	70	90%
Present work	Methyl Green	10	SnS-NPs-AC	0.2	50	99 %

and or hydrophilic forces. Besides, for the role of activated carbon can be said that the most possible mechanism is H-bonding between N, and O atoms of understudy dyes and H atom of COOH and OH group of activated carbon.

Comparison with literature

Comparison of performance of the proposed method and this adsorbent with other methods and some adsorbents are summarized in Table 3. Accordingly, the SnS-NPs-AC is superior to all other applied adsorbent in terms of satisfactory removal performance for methyl green. The results indicated that the combination of magnetite stir bar with SnS-NPs-AC causes accelerated of mass transfer rate in less contact time (<40 min), as well as coupled metallic nanoparticles with AC cause the increase in the adsorption capacity [52-55].

CONCLUSIONS

Tin sulfide-based nanoparticles were prepared and then coated on activated carbon and used for methylene green dye removal from aqueous solution. Both adsorbents were characterized by TEM, UV-Vis spectrometry and FT-IR analysis. Effects of various operating parameters including, solution pH, initial dye concentration, contact time and adsorbent dosage on the extent of dye adsorption were investigated and the results were analyzed. The optimum dosage, initial Methylene green concentration, pH and contact time for [SnS-NP-AC] were obtained to be 0.2 g, 10 mg/L, pH 8 and 50 min, respectively. It was seen that [SnS-NP-AC] was effective adsorbent for the removal of Methylene green from aqueous solution. The high Methylene green removal using both adsorbents, showed their applicability to remove the said dye in short equilibrium time (less than 50 min). The equilibrium and kinetic studies were investigated for the adsorption process. The isotherm models such as Langmuir, Freundlich, D-R, and Temkin were evaluated and the equilibrium data were best described by the Langmuir model. The process kinetics can be successfully fitted to the pseudo-second-order kinetic model.

Received : Feb. 1, 2018 ; Accepted :Jul. 30, 2018

REFERENCES

[1] Robinson T., Mcmullan G., Marchant R., Nigam P., Remediation of Dyes in Textile Effluent: a Critical Review on Current Treatment Technologies with a Proposed Alternative, *Bioresour. Technol.*, **77**: 247–255 (2001).

[2] Aksu Z., Application of Biosorption for the Removal of Organic Pollutants: A Review, *Proc. Biochem.* **40**: 997–1026 (2005).

[3] Vijayaraghavan K., Yun Y.S., Biosorption of C.I. Reactive Black 5 from Aqueous Solution Using Acid-Treated Biomass of Brown Seaweed Laminaria sp., *Dyes Pigments*, **76**: 726–732(2008).

[4] Moussavi G., Mahmoudi M., Removal of Azo and Anthraquinone Reactive Dyes from Industrial Wastewaters Using MgO Nanoparticles, *J. Hazard. Mater.*, **168**: 806–812(2009).

[5] Apostol L.C., Pereira L., Pereira R., Gavrilescu M., Alves M.M., Biological Decolorization of Xanthene Dyes by Anaerobic Granular Biomass, *Biodegradation*, **23**: 725–737(2012).

[6] Shokri A., Application of Electrocoagulation Process for the Removal of Acid Orange 5 in Synthetic Wastewater. *Iran. J. Chem. Chem. Eng. (IJCCE)*, **38**(2): 113-119 (2019).

[7] Türgay O., Ersz G., Atalay S., Forss J., Welander U., The Treatment of Azo Dyes Found in Textile Industry Wastewater by Anaerobic Biological Method and Chemical Oxidation, *Sep. Purif. Technol.*, **79**: 26-33 (2011).

[8] Zavastin D.E., Gherman S., Cretescu I., Removal of Direct Blue Dye from Aqueous Solution Using New Polyurethane–Cellulose Acetate Blend Micro-Filtration Membrane, *Rev. Chim.*, **63**: 1075-1078 (2012).

[9] Kamranifar M., Naghizadeh A., Montmorillonite Nanoparticles in Removal of Textile Dyes from Aqueous Solutions: Study of Kinetics and Thermodynamics, *Iran. J. Chem. Chem. Eng. (IJCCE)*, **36**: 127-137 (2017).

[10] Madhusudan P., Zhang J., Cheng B., Liu G., Photocatalytic Degradation of Organic Dyes with Hierarchical $Bi_2O_2CO_3$ Microstructures Under Visible-Light, *Cryst. Eng. Comm.*, **15**: 231-240 (2013).

[11] Lee C.-R., Kim H.-S., Jang I.-H., Im J.-H., Park N.-G., Pseudo First-Order Adsorption Kinetics of N719 Dye on TiO_2 Surface, *ACS Appl. Mater. Interf.* **3**: 1953-1957 (2011).

[12] Liu G., Hou M., Song J., Jiang T., Fan H., Zhang Z., Han B., Immobilization of Pd Nanoparticles with Functional Ionic Liquid Grafted onto Cross-Linked Polymer for Solvent-Free Heck Reaction, *Green Chem.*, **12**: 65-69 (2010).

[13] Pal S., Mal D., Singh R.P., Cationic Starch: An Effective Flocculating Agent, *Carbohydr. Polym.*, **59**: 417-423 (2005).

[14] Ma Y., Zheng Y., Chen J.P., A Zirconium Based Nanoparticle for Significantly Enhanced Adsorption of Arsenate: Synthesis, Characterization and Performance, *J. Colloid. Int. Sci.*, **354**: 785-792 (2005).

[15] Chen Y.H., Synthesis, Characterization and Dye Adsorption of Ilmenite Nanoparticles, *J. Non. Cryst. Solid.*, **357**: 136-139 (2011).

[16] Qiu H., Sawada T., Jiang S., Ihara H., New Strategy for Drastic Enhancement of Selectivity *Via* Chemical Modification of Counter Anions in Ionic Liquid Polymer Phase, *Chemical Communications*, **46**: 8740-8742 (2010).

[17] Qiu H., Takafuji M., Sawada T., Liu X., Jiang S., Ihara H., Ionic Liquid (Molten Salt) Phase Organometallic Catalysis, *Chemical Reviews*, **102**: 3667-3692 (2002).

[18] Zhong Y., Qiu X., Chen D., Li N., Xu Q., Li H., Lu H., Flexible Electrospun Carbon Nanofiber/Tin (IV) Sulfide Core/Sheath Membranes for Photocatalytically Treating Chromium (VI)-Containing Wastewater, *J. ACS Appl. Mater. Interfaces*, **8**: 28671-28677 (2016).

[19] Chen Q., Lu F., Xia Y., Wang H., Kuang X., Lithiation-Assisted Exfoliation and Reduction of SnS_2 to SnS Decorated on Lithium-Integrated Graphene for Efficient Energy Storage, *J. Mater. Chemi. A*, **5**: 4075-4083 (2017).

[20] Bian X., Xiaofeng L., Yanpeng X., Chengcheng Z., Lirong K., Ce W., A Facile One-Pot Hydrothermal Method to Produce SnS_2/Reduced Graphene Oxide with Flake-on-Sheet Structures and Their Application in the Removal of Dyes from Aquaes Solution, *J. Coll. Interface Sci.*, **406**: 37-43 (2013).

[21] Xiong X., Yang C., Wang G., Lin Y., Ou X., Wang J.H., Huang K., SnS Nanoparticles Electrostatically Anchored on Three-Dimensional N-Doped Graphene as an Active and Durable Anode for Sodium-Ion Batteries, *Energ. Enviro. Sci.*, **10**: 1757-1763 (2017).

[22] Fuerhacker M., Haile T.M., Kogelnig D., Stojanovic A., Keppler B., Application of Ionic Liquids for the Removal of Heavy Metals from Wastewater and Activated Sludge, *Water Sci. Technol.*, **65**: 1765–1773 (2012).

[23] Gharehbaghi M., Shemirani F., A Novel Method for Dye Removal: Ionic Liquid-Based Dispersive Liquid–Liquid Extraction (IL-DLLE), *Clean. Soil. Air Water*, **40**: 290–297 (2012).

[24] Poursaberi T., Hassanisadi M., Magnetic Removal of Reactive Black 5 from Wastewater Using Ionic Liquid Grafted-Magnetic Nanoparticles, *Clean Soil Air Water*, **41**: 1208-1215 (2013).

[25] Ghaedi M., Ghaedi A.M., Negintaji E., Ansari A., Vafaei A., Rajabi M., Random Forest Model for Removal of Bromophenol Blue Using Activated Carbon Obtained from Astragalus Bisulcatus Tree, *J. Ind. Eng. Chem.*, **20**: 1793-1803 (2014).

[26] Assefi P., Ghaedi M., Ansari A., Habibi M.H., Momeni M.S., Artificial Neural Network Optimization for Removal of Hazardous Dye Eosin Y from Aqueous Solution Using Co_2O_3-NP-AC: Isotherm and Kinetics Study, *J. Ind. Eng. Chem.*, **20**: 2905-2913 (2014).

[27] Ghaedi M., Ansari A., Habibi M.H., A.R. Removal of Malachite Green from Aqueous Solution by Zinc Oxide Nanoparticle Loaded on Activated Carbon: Kinetics and Isotherm Study, *J. Ind. Eng. Chem.*, **20**: 17-28 (2014).

[28] Ravanan M., Ghaedi M., Ansari A., Taghizadeh F., Elhamifar D., Comparison of the Efficiency of Cu and Silver Nanoparticle Loaded on Supports for the Removal of Eosin Y from Aqueous Solution: Kinetic and Isotherm Study, *Spectrochim. Acta A*, **123**: 467-472 (2014).

[29] Wang X., Zhu N., Yin B., Preparation of Sludge-Based Activated Carbon and Its Application in Dye Wastewater Treatment, *J. Hazard. Mater*., **153**: 22–27 (2008).

[30] Tan I.A.W., Ahmad A.L., Hameed B.H., Adsorption of Basic Dye on High-Surface-Area Activated Carbon Prepared from Coconut Husk: Equilibrium, Kinetic and Thermodynamic Studies, *J. Hazard. Mater*. **154**: 337–346 (2008).

[31] Ghaedi M., Ansari A., Sahraei R., ZnS: Cu Nanoparticles Loaded on Activated Carbon as Novel Adsorbent for Kinetic, Thermodynamic and Isotherm Studies of Reactive Orange 12 and Direct Yellow 12 and Direct Yellow 12 Adsorption, *Spectrochim. Acta A*, **114**: 687-694 (2013).

[32] Ghaedi M., Comparison of Cadmium Hydroxide Nanowires and Silver Nanoparticles Loaded on Activated Carbon as New Adsorbents for Efficient Removal of Sunset Yellow: Kinetics and Thermodynamic Study, *Spectrochim. Acta A*, **94**: 346 346 (2012).

[33] Ghaedi M., Hossainian H., Montazerozohori M., Shokrollahi A., Shojaipour F., Soylak M., Purkait M., A Novel Acorn Based Adsorbent for the Removal of Brilliant Green, *Desalination*, **281**: 226- (2011).

[34] Tempkin M.J., Pyzhev V., Recent Modifications to Langmuir Isotherms, *Physiocho chimica. Acta USSR*, **12**: 217-222 (1940).

[35] Ghaedi M., Sadeghian B., Amiri Pebdani A., Sahraei R., Daneshfar A., Duran C., Kinetics, Thermodynamics and Equilibrium Evaluation of Direct Yellow 12 Removal by Adsorption onto Silver Nanoparticles Loaded Activated Carbon, *Chem. Engi. J.*, **187**: 133-141 (2012).

[36] Dubinin M.M., The Potential Theory of Adsorption of Gases and Vapors for Adsorbents with Energetically Nonuniform Surfaces, *Chemical Reviews*, **60**: 235- (1960).

[37] Dubinin M.M., Zhurnal Fizicheshoi Khimii Modern State of the Theory of Volume Filling of Micropore Adsorbents During Adsorption of Gases and Steams on Carbon Adsorbents, *Pure Appl. Chem.*, **39**: 1305-1317 (1965).

[38] Radushkevich L.V., Potential Theory of Sorption and Structure of Carbons, *Zhurnal Fizicheshoi Khimii*, **23**: 1410-1420 (1949).

[39] Lagergren S., Zur Theorie Der Sogenannten Adsorption Geloster Stoffe, *Handlingar*, **24**: 1-39 (1898).

[40] Chien S.H., Clayton W.R., Application of Elovich Equation to the Kinetics of Phosphate Release and Sorption in Soils 1, *Soil Sci. Soc. Amer. J.*, **44**, 265-268 (1980).

[41] Ghaedi M., Ghaedi A.M., Hosseinpour M., Ansari A., Habibi M.H., Asghari A.R., Solar Light Photocatalytic Degradation of Malachite Green by Hydrothermally Synthesized Strontium Arsenate Nanomaterial through Response Surface Methodology, *J. Ind. Eng. Chem.*, **644**: 221-227 (2018).

[42] Ruhan A.A., Ahmet S., Mustafa T., Equilibrium, Thermodynamic and Kinetic Studies on Biosorption of Pb (II) and Cd (II) from Aqueous Solution by Macrofungus (Lactarius scrobiculatus) Biomass, *Chem. Eng. J.*, **151**: 255-261 (2009).

[43] Weber W.J., Morris J.C., Kinetics of Adsorption on Carbon from Solution, *Am. Soc. Civil Eng.*, **89**: 31-60 (1963).

[44] Sari A., Tuzen M., Kinetic and Equilibrium Studies of Biosorption of Pb (II) and Cd (II) from Aqueous Solution by Macrofungus (Amanita rubescens) Biomass, *J. Hazard. Mater*., **164**: 1004-1011 (2009).

[45] Dogan M., Abak H., Alkan M., Adsorption of Methylene Blue onto Hazelnut Shell: Knetics, Mechanism and Activation Parameters, *J. Hazard. Mater*., **164**: 172-181 (2009).

[46] Crini G., Gimbert F., Robert C., Martel B., Adama O., The Removal of Basic Blue 3 from Aqueous Solutions by Chitosan-Based Adsorbent: Batch Studies, *J. Hazard. Mater*., **153**: 96-106 (2008).

[47] A. Sari, M. Tuzen, Biosorption of Total Chromium from Aqueous Solution by Red Algae (Ceramium virgatum): Equilibrium, Kinetic and Thermodynamic studies. *J. Hazard. Mater*. 160: 349-355 (2008).

[48] Chiou M.S., Chuang G.S., Competitive Adsorption of Dye Metanil Yellow and RB15 in Acid Solutions on Chemically Cross-Linked Chitosan Beads *Chemosphere*, **62**: 731-740 (2006).

[49] Li K.Q., Wang X.H., Adsorptive Removal of Pb (II) by Activated Carbon Prepared from Spartina Alterniflora: Equilibrium, Kinetics and Thermodynamics, *Bioresour. Technol*., **100**: 2810-2815 (2009).

[50] Tseng R.L., Mesopore Control of High Surface Area NaOH-Activated Carbon, *J. Colloid Interface Sci.*, **303**: 494-502 (2006).

[51] Chen S., Zhang J., Zhang C., Yue Q., Li Y., Li C., Equilibrium and Kinetic Studies of Methyl Orange and Methyl Violet Adsorption on Activated Carbon Derived from Phragmites Australis, *Desalination*, **252**: 149-156 (2010).

[52] Tang X., Li Y., Chen R., Min F., Yang J., Dong Y., Evaluation and Modeling of Methyl Green Adsorption from Aqueous Solutions Using Loofah Fibers, *Korean J. Chem. Eng.*, **32**: 125-131 (2015).

[53] Bahgat M., Farghali A.A., El Rouby W., Khedr M., Mohassab-Ahmed M.Y., Adsorption of Methyl Green Dye onto Multi-Walled Carbon Nanotubes Decorated with Ni Nanoferrite, *App. Nanosci.*, **3**: 251-261 (2013).

[54] Dos Reis L.G.T., Robaina N.F., Pacheco W.F., Cassella R.J., Separation of Malachite Green and Methyl Green Cationic Dyes from Aqueous Medium by adsorption on Amberlite XAD-2 and XAD-4 Resins Using Sodium Dodecylsulfate as Carrier, *Chem. Eng. J.*, **171**: 532-540 (2011).

[55] Shouman M., Khedr S., Removal of Cationic Dye from Aqueous Solutions by Modified Acid-Treated Pomegranate Peels (PUNICA GRANATUM): Equilibrium and Kinetic Studies, *Asian J. App. Sci.*, **3**: 1-15 (2015).